

微生物学报 *Acta Microbiologica Sinica*

54(7):803-812; 4 July 2014

ISSN 0001-6209; CN 11-1995/Q

http://journals.im.ac.cn/actamicrocn

doi: 10.13343/j.cnki.wsxb.2014.07.011

受低毒病毒调控的板栗疫病菌总蛋白质组学

王金子^{1,2}, 卢立丹¹, 杨彦彦¹, 陈琦¹, 陈保善^{1,3*}

广西大学,¹ 生命科学与技术学院,² 农学院, 广西 南宁 530005

³ 亚热带农业生物资源保护与利用国家重点实验室, 广西 南宁 530005

摘要: 【目的】为解析低毒病毒调控板栗疫病菌生理性状和致病性的机制, 在总蛋白质组水平上寻找受病毒侵染调控的宿主蛋白及其编码基因。【方法】使用双向电泳方法对野生型菌株 EP155 和受低毒病毒感染的菌株 EP713 进行差异蛋白质组分析, 同时, 对差异表达蛋白质编码基因的 mRNA 水平进行定量分析。【结果】共找到 71 个因病毒侵染而发生差异表达的蛋白质点, 分别属于 58 种不同蛋白质。以 EP155 为对照, 表现为上调的 19 个, 下调的 52 个, 主要涉及能量代谢, 蛋白质、核酸和碳水化合物代谢, 信号传导以及压力应激和氧化还原反应。对 10 个受病毒调控的蛋白的编码基因进行了 mRNA 水平定量, 其中 7 个基因受病毒感染后的 mRNA 水平变化与蛋白水平变化趋势一致, 3 个基因的 mRNA 水平变化与蛋白水平变化趋势不相符, 表明低毒病毒对板栗疫病菌不同基因的调控可以发生在不同的调控层面上。【结论】低毒病毒的侵染弱化了宿主 TCA 循环的能量流动, 调控了宿主体内的甲基化过程及真菌致病因子的表达。

关键词: 板栗疫病菌, 低毒病毒, 比较蛋白质组

中图分类号: Q93 **文章编号:** 0001-6209(2014)07-0803-10

低毒病毒/板栗疫病菌 (*hypovirus/Cryphonectria parasitica*) 系统是目前发展起来的几种有效研究病毒-宿主相互作用的模式系统之一^[1]。板栗疫病菌在 20 世纪初曾经造成北美板栗树林的毁灭性破坏, 是一种非常重要的植物致病真菌^[2]。低毒病毒是一类无衣壳的 RNA 病毒, 能够侵染板栗疫病的病原真菌—板栗疫病菌。病毒的感染能使宿主产生持久的表型变化, 包括抑制色素分泌和降低分生孢子的生成量, 同时显著改变真菌致病力即产生低毒力现象^[1]。通过胞质融合在菌株之间传递低毒力, 已被

应用于板栗疫病的生物防治上, 并取得了一定的成功^[3-4]。

低毒病毒侵染对宿主病菌造成表型变化, 暗示着宿主体内代谢途径受到病毒的调控而发生改^[5-6]。随后的研究证实了宿主体内几条重要的信号传导途径, 包括 G 蛋白介导的 cAMP 信号传导途径^[5, 7-9]、MAPK 信号传导途径^[10-12] 和钙调蛋白信号传导途径都受到病毒的调控^[9, 13]。近年来, 有关板栗疫病菌蛋白质组学的研究也逐渐开展起来, 其中在受低毒病毒侵染的囊泡蛋白质组

基金项目: 国家自然科学基金面上项目 (31170137, 31370173); 国家杰出青年科学基金 (39925003)

* 通信作者。Tel: +86-771-3225260; Fax: +86-771-3237873; E-mail: chenyaaj@gxu.edu.cn

作者简介: 王金子 (1982-), 男, 黑龙江省齐齐哈尔人, 博士, 主要从事分子病毒学和蛋白质组学方面的研究。E-mail: wangzi4444@163.com

收稿日期: 2013-11-18; **修回日期:** 2014-03-09

中,发现了低毒病毒蛋白 p48 新的加工形式,同时明确了囊泡作为病毒载体在宿主体内运输起到的重要作用^[14]。之前对板栗疫病菌总蛋白组的研究中,已有 30 个受低毒病毒侵染发生改变的宿主蛋白质被发现,但由于实验设计和鉴定的蛋白质信息过少,尚不能就病毒侵染对宿主造成的影响进行合理的解释^[15]。本文使用双向电泳技术对板栗疫病菌野生型菌株 EP155 和低毒病毒感染株 EP713 的总蛋白质组进行比较分析,发现病毒调控宿主初级代谢途径多个关键酶和真菌致病因子的表达。

1 材料和方法

1.1 主要试剂和仪器

本试验使用的试剂及设计合成的特异性引物,均购自生工生物工程(上海)股份有限公司。反转录试剂盒为 Thermo Scientific 公司旗下 Fermentas 系列产品,定量 PCR 试剂盒 SuperReal PreMix 购自天根生化科技(北京)有限公司。双向电泳平台及相关试剂耗材采用 GE Healthcare 公司产品。

1.2 真菌培养条件

本试验所涉及板栗疫病菌菌株均来源于美国马里兰大学 Nuss 实验室,为本实验室保存。EP155 (ATCC 38755) 是板栗疫病菌野生强毒株,EP713 (ATCC 52571) 是携带低毒病毒 CHV1-EP713 的低毒菌株。经活化的 EP55 和 EP713 菌种接种于铺有玻璃纸的马铃薯葡萄糖琼脂培养基(PDA)上,在实验室桌面条件(23-25℃,12h 光照/12h 黑暗),培养 7 d。

1.3 真菌总蛋白质样品的提取

将菌体于液氮中研磨粉碎,加入 10 倍体积预冷丙酮(含 10% TCA,0.07% β -mercaptoethanol)振荡悬浮,置 -20℃ 沉淀过夜后,在 4℃、20000 × g 离心 30 min,收集沉淀并重悬于 6 倍体积预冷丙酮。-20℃ 静置 1 h 后,在 4℃、20000 × g 离心 30 min,收集沉淀,重复上述沉淀离心步骤 2 次。将获得的最后沉淀进行真空浓缩 10 min,彻底除去残留丙酮。将蛋白质干粉重悬于 1 mL 通用裂解液(7.5 mol/L 尿素,2.5 mol/L 硫脲,12.5% 甘油,50 mmol/L Tris,2.5% *n*-辛基葡萄糖苷,6.25 mmol/L TCEP,0.17% 蛋白酶抑制剂),在冰浴下

用超声波处理(200 w,12 s;间隔 15 s,工作 5 个循环)。在 4℃、20000 × g 离心 30 min,除去沉淀,上清液分装冻存于 -80℃ 待用。样品蛋白浓度用 2D Quant 试剂盒(GE Healthcare)定量。

1.4 双向电泳及凝胶图像处理

选用 24 cm pH3-10 和 pH4-7 线性胶条,使用 Ettan IPGphor 3 IEF System 进行等电聚焦。上样量 600 μ g,等电聚焦温度为 20℃,每根胶条电流不超过 50 μ A。先在 30 V 和 60 V 各运行 6 h 进行低电压水化,然后在 500 V 和 1000 V 各运行 1 h,再在 1000-8000 V 梯度上升 1 h,最后在 8000 V 运行 8 h。胶条进行平衡处理后,在 Ettan DALTsix 垂直板电泳系统(GE Healthcare)进行第二向 SDS-PAGE,电泳条件为 10 mA/gel 保持 30 min,然后在 20 mA/gel 继续电泳,直到溴酚蓝前沿到达凝胶底部。每个样品的双向电泳重复 3 次。采用质谱兼容银染显色法对凝胶进行染色^[16],用 ImageScanner 扫描仪在 300 dpi 分辨率下对凝胶进行扫描。凝胶图像分析软件版本为 ImageMaster 5.0。

1.5 蛋白质胶内酶解及萃取

胶内酶解及萃取采用 Gharahdaghi 等建立的标准方法^[17],略有改动。从凝胶上挖下约(2-4) mm × (2-4) mm 的小胶粒,过夜酶解后,加入萃取液(0.1% 三氟乙酸,50% 乙腈)并进行超声波萃取。离心后收集萃取液,真空浓缩抽干后,再用 1 μ L 萃取液复溶肽段沉淀。

1.6 质谱鉴定

取 0.5 μ L 肽段溶液点样于 MALDI 板上,加入等体积 CHCA 基质。待样品结晶后,用 ABI 4800 plus 质谱仪进行串联质谱鉴定。PMF 质量扫描范围为 800-3500 Da。选择强度最高的 5 个肽段进行二级质谱分析。激光强度和信噪比阈值均使用仪器默认设置。使用 GPS ExplorerTM 软件将实际质谱鉴定数据与板栗疫病菌全基因组数据库信息([http://genomeportal.jgi-psf.org/Crypa1/Crypa1.download.ftp.html](http://genomeportal.jgi-psf.org/Crypa1/Crypa1.download ftp.html))进行搜索和比对。

1.7 定量 RT-PCR

提取板栗疫病菌 RNA^[18],使用特异引物(表 1)、Fermentas 反转录试剂盒和 TIANGEN SuperReal PreMix 定量试剂盒对目标基因进行反转录和定量 PCR 分析。以 18S rRNA 作为内参基因,用 $2^{-\Delta\Delta Ct}$ 法进行基因相对表达量分析^[19]。

表 1. 供试验研究使用的引物
Table 1. Primers used in the test

primer	sequence (5' → 3')
43908-F	GAAGAAGTACATGGCCACCTC
48013-F	CTGTGCCGTGGTAATTTTGC
66481-F	CGCCCAAGTGGCAAGATCAC
81890-F	TCTACAGTCTCTCGGTGAGGC
102434-F	ACCCCCAGCATCAAGCAGATC
90806-F	CACATCCGGATCGGCGATATC
98577-F	CCACAAGCACGCCAGAGTAAG
102068-F	CCACCTACCCTATGCAGTGCTC
72349-F	GAGGCTCTCAGCCACCTAGAAG
45332-F	AGGAAGCCTACGTGAGCACC
18s-F	TCTCGAATCGCATGGCCT
18s-R	TTACCCGTTGTAACACCGC
43908-R	TAGTACCCATCACGAGGCCAC
48013-R	TGGAGAGGCTCGAAACCACC
66481-R	GGATGTCTTGGCATTCTCGC
81890-R	TCGACGGCCTTGCTAGACTC
102434-R	AACCTTGTGGCGCCATC
90806-R	CCTGGAGCTGCTTGGTGAAC
98577-R	GCATTTATCGCCACCACGTG
102068-R	AGATGAACCTTGGCGTGACC
72349-R	AATTGCCCGCCGAAAACG
45332-R	AAAGCTCGTGCCGGCCTC

2 结果和分析

2.1 总蛋白质双向电泳

双向电泳凝胶图谱显示, 板栗疫病菌总蛋白主要集中在 pH 4-7 之间, 不同批次制样的蛋白质点重现性好, 适合于差异比较分析。以野生强毒株 EP155 为基准, 低毒病毒侵染菌株 EP713 具有 2.5 倍以上表达差异的蛋白质点共有 71 个, 其中上调 19 个, 下调 52 个(图 1)。

2.2 差异表达蛋白质谱鉴定结果

串联质谱鉴定双向电泳中出现的 71 个差异表达蛋白质点, 其中 65 个蛋白点得到有效鉴定, 共得到 58 种蛋白质信息(表 2)。生物信息学分析发现, 这些蛋白质主要属于能量代谢, 蛋白质、核酸和碳水

化合物代谢, 信号传导, 压力应激和氧化还原反应, 其中包括已经从转录组水平研究确认为受低毒病毒调控差异表达的 *gpd1*^[20]、*epr1*^[21] 和 *cyp1*^[22] 等。

2.3 差异表达蛋白质编码基因的转录水平变化

在随机挑选的 10 个差异表达蛋白质编码基因中, 7 个基因(基因组数据库编号分别为 66481、102434、98577、43908、90806、45332 和 72349)在转录水平的表达趋势与蛋白质水平趋势一致; 3 个基因(基因组数据库编号分别为 81890、102068 和 48031)没有明显变化(变化倍数小于 1.5)或呈现反向变化(图 2)。

3 讨论

3.1 低毒病毒侵染对宿主糖酵解和三羧酸循环的影响

如图 1 所示, 烯醇酶(enolase, 编号 160)、3-磷酸甘油醛脱氢酶(glyceraldehyde-3-phosphate dehydrogenase, 编号 189)和葡萄糖磷酸变位酶(phosphoglucosmutase, 编号 107)受低毒病毒影响均发生显著下调, 而乙醛脱氢酶(aldehyde dehydrogenase, 编号 40、49)则显著上调。这四种酶表达水平的变化均会影响进出三羧酸(TCA)循环的乙酰辅酶 A(acetyl-CoA)和草酰乙酸(oxaloacetate)的水平, 从而使整个 TCA 循环和能量代谢发生改变^[25]。同时, 来自蔗糖代谢途径的 α -葡糖苷酶(neutral alpha-glucosidase 编号 131、132)和氨基和核苷酸糖代谢途径的乙酰氨基葡萄糖焦磷酸化酶(UDP-N-acetylglucosamine pyrophosphorylase, 编号 19、20、21)的表达下调, 间接影响 6-磷酸葡萄糖(glucose-6-phosphate)和 6-磷酸果糖(fructose-6-phosphate)的产量, 也对 TCA 循环产生同样的影响。这一现象与之前对板栗疫病菌的初级代谢组研究所观察到的结果完全吻合^[26]。将这些受病毒调控的宿主蛋白与糖酵解和三羧酸循环关联途径进行耦合分析, 可以看出低毒病毒的侵染改变了宿主代谢和能量流向(图 3)。由此推测, 为保障病毒在宿主体内的复制和运输提供动力, 病毒侵染在弱化宿主关键代谢途径的同时, 触发了宿主体内代谢补偿机制, 例如, 增加能量的利用效率。这一观点与之前观察到的病毒利用宿主囊泡系统进行细胞内运输, 需要额外能量和运输空间的结论相一致^[14]。

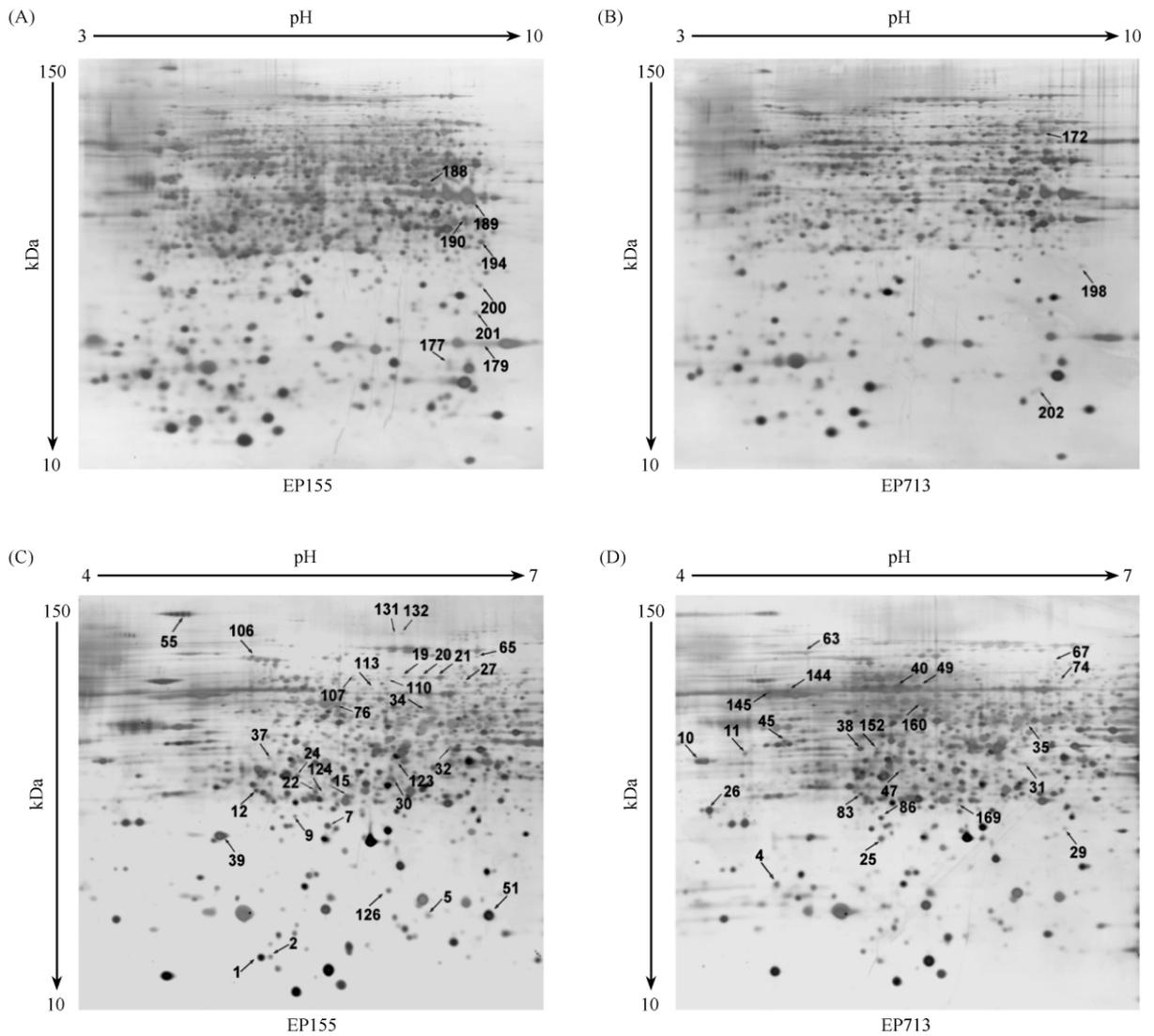


图 1. 双向电泳分析板栗疫病菌 EP155 和 EP713 总蛋白

Figure 1. 2-DE analysis of total protein from *C. parasitica* strains EP155 and EP713. Proteins were extracted from fungal cultures grown on PDA medium for 7 days. Protein samples of 600 μg (from the wild type strain EP155 and the hypovirus-infected strain EP713) were isoelectrically focused using pH 3–10 (A, B) and pH 4–7 (C, D) IPG strips and subsequently separated by 12.5% SDS-PAGE.

表 2. EP155 与 EP713 之间的差异表达蛋白质名录
Table 2. List of differentially expressed proteins between EP155 and EP713

spot ID ^a	protein name	accession number ^b	ratio ^c	EST evidence ^d	regulation ^e
123	2-amino-3-carboxymuconate-6-semialdehy decarboxylase	101881	-10 ⁶	Ref ^[23-24]	R \rightarrow P \downarrow
198	Acetoin (diacetyl) reductase	36707	-2.5	Ref ^[24]	R \rightarrow P \downarrow
40	Aldehyde dehydrogenase	34827	2.5	Ref ^[23-24]	R \rightarrow P \uparrow
49	Aldehyde dehydrogenase	34827	3.6	Ref ^[23-24]	R \rightarrow P \uparrow
144	ATP synthase subunit beta, mitochondrial	88762	10 ⁶	Ref ^[23-24]	R \uparrow [24], P \uparrow
31	ATP synthase subunit gamma	92423	-3.2	Ref ^[24]	R \downarrow [24], P \downarrow
67	Bifunctional purine biosynthesis protein	42705	-3.4	Ref ^[24]	R \rightarrow P \downarrow
110	Bifunctional purine biosynthesis protein	42705	-10 ⁶	Ref ^[24]	R \rightarrow P \downarrow

续表 2

spot ID ^a	protein name	accession number ^b	ratio ^c	EST evidence ^d	regulation ^e
113	CDP-alcohol phosphatidyltransferase class-I family protein	81875	-10 ⁶	Ref [23-24]	R↔ P ↓
10	Elongation factor 1-beta	102227	4.9	Ref [23-24]	R↔ P ↑
145	Endothiapepsin	100383	10 ⁶	Ref [23-24]	R ↓ [18] [21], P ↑
160	Enolase	103155	-2.5	Ref [23-24]	R ↓ [24], P ↓
39	Eukaryotic translation initiation factor 5A-2	102068	-2.7	Ref [23-24]	R ↓ [24], P ↓
189	Glyceraldehyde-3-phosphate dehydrogenase	101684	-10 ⁶	Ref [23-24]	R ↑ [24] [20], P ↓
29	GTP-binding nuclear protein GSP1/Ran	43908	-3.3	Ref [23-24]	R ↑ [24] [18], P ↓
37	Heat shock protein 30	103088	2.5	Ref [23]	R↔ P ↑
63	Heat shock protein 70	107004	2.5		P ↑
126	Nascent polypeptide-associated complex subunit beta	102329	-10 ⁶	Ref [23-24]	R ↓ [24], P ↓
11	Nascent polypeptide-associated complex subunit alpha	81890	4.6	Ref [24]	R↔ P ↑
131	Neutral alpha-glucosidase	88086	-10 ⁶		P ↓
132	Neutral alpha-glucosidase	88086	-10 ⁶		P ↓
179	Peptidyl-prolyl cis-trans isomerase, mitochondrial	55987	-14	Ref [23-24]	R ↑ [24] [22], P ↓
25	Peroxiredoxin	68536	2.9		P ↑
107	Phosphoglucomutase	102434	-10 ⁶	Ref [23-24]	R ↓ [18], P ↓
24	Probable 6-phosphogluconolactonase	59149	-10 ⁶		P ↓
190	Probable rhamnose biosynthetic enzyme 1	107766	-3.5	Ref [23-24]	R ↓ [18], P ↓
27	Probable T-complex protein 1 subunit beta	99165	-10 ⁶	Ref [23-24]	R↔ P ↓
106	Protein disulfide-isomerase MPD1	98577	-10 ⁶	Ref [23-24]	R↔ P ↓
26	Protein wos2	101651	3.4	Ref [23-24]	R↔ P ↑
83	Putative agmatinase 1	93897	-2.9	Ref [23-24]	R ↓ [18], P ↓
34	Putative dioxygenase	97903	-10 ⁶	Ref [23-24]	R ↑ [18], P ↓
65	Putative glycyl-tRNA synthetase	87412	-2.5		P ↓
47	Rhamnolipids biosynthesis 3-oxoacyl-[acyl-carrier-protein] reductase	64761	2.5	Ref [23-24]	R↔ P ↑
38	S-adenosylmethionine-dependent methyltransferase	72349	4.2		P ↑
86	S-adenosylmethionine-dependent methyltransferase	45332	3.7		P ↑
152	S-adenosylmethionine-dependent methyltransferase	72349	10 ⁶		P ↑
202	Single-stranded DNA-binding protein RIM1, mitochondrial	66481	-2.7		P ↓
200	Translation machinery-associated protein 20	69225	-10 ⁶	Ref [23]	R↔ P ↓
19	UDP-N-acetylglucosamine pyrophosphorylase	107213	-10 ⁶	Ref [23-24]	R↔ P ↓
20	UDP-N-acetylglucosamine pyrophosphorylase	107213	-10 ⁶	Ref [23-24]	R↔ P ↓
21	UDP-N-acetylglucosamine pyrophosphorylase	107213	-10 ⁶	Ref [23-24]	R↔ P ↓
45	UPF0010 protein	81476	10 ⁶	Ref [23-24]	R↔ P ↑
74	UTP-glucose-1-phosphate uridylyltransferase	42588	-2.5	Ref [23-24]	R ↓ [18], P ↓
177	Woronin body major protein, HEX-1	90806	-2.5	Ref [23-24]	R↔ P ↓
1	Uncharacterized protein	36895	-2.8		P ↓
2	Uncharacterized protein	74053	-3.2	Ref [24]	
4	Uncharacterized protein	70844	3.8		P ↑
5	Uncharacterized protein	102688	-10 ⁶	Ref [23-24]	R ↓ [24], P ↓
7	Uncharacterized protein	104362	-10 ⁶	Ref [23-24]	R↔ P ↓
9	Uncharacterized protein	99352	-10 ⁶	Ref [23-24]	R↔ P ↓
12	Uncharacterized protein	62371	-3.5		P ↓
15	Uncharacterized protein	50824	-10 ⁶	Ref [24]	R↔ P ↓
22	Uncharacterized protein	75077	-4.2		P ↓
30	Uncharacterized protein	73459	-3.1	Ref [23-24]	R ↑ [18], P ↓
32	Uncharacterized protein	57922	-10 ⁶	Ref [24]	R↔ P ↓
35	Uncharacterized protein	53588	10 ⁶	Ref [24]	R↔ P ↑
51	Uncharacterized protein	102688	-17.6	Ref [23-24]	R ↓ [24], P ↓
55	Uncharacterized protein	107358	-2.5	Ref [24]	R↔ P ↓

续表 2

spot ID ^a	protein name	accession		EST evidence ^d	regulation ^e
		number ^b	ratio ^c		
76	Uncharacterized protein	48013	-4.7	Ref ^[24]	R↔ P↓
124	Uncharacterized protein	106447	-10 ⁶	Ref ^[24]	R↔ P↓
169	Uncharacterized protein	96317	-2.5	Ref ^[23]	R↔ P↓
172	Uncharacterized protein	88910	-3.5	Ref ^[23-24]	R↓ ^[18] , P↓
188	Uncharacterized protein	94574	-2.5	Ref ^[23-24]	R↔ P↓
194	Uncharacterized protein	104871	-10 ⁶	Ref ^[23-24]	R↑ ^[24] ^[18] , P↓
201	Uncharacterized protein	85077	-10 ⁶	Ref ^[23-24]	R↑ ^[24] , P↓
3			3.2		P↑
81			-4.1		P↓
116			-10 ⁶		P↓
122			-10 ⁶		P↓
161			10 ⁶		P↑
193			-10 ⁶		P↓

a, differentially expressed protein spots referred in Figure 1. b, accession number of the identified protein in *C. parasitica* database 1.0; c, with hypovirus-free strain EP155 as reference, a positive value means up regulation and negative value down regulation by hypovirus infection; a value of 10⁶ means that the protein spot appears only in EP713; and a value of -10⁶ means that the spot appears only in EP155; d, found in the EST library of *C. parasitica*; e, regulation of host genes by hypovirus infection. R represents transcriptional level and P protein level. “-” means not reported “↑” up-regulated, and “↓” down-regulated by hypovirus.

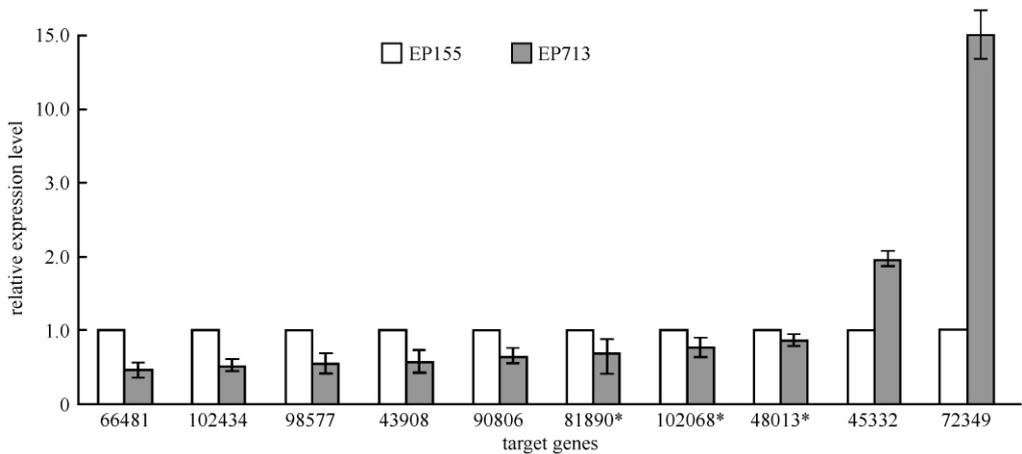


图 2. 荧光定量 RT-PCR 分析在蛋白质水平上受低毒病毒调控的 10 个宿主基因的 mRNA 表达量

Figure 2. Real-time RT-PCR quantification of mRNA level of ten host genes regulated by hypovirus infection at protein level. The gene transcript levels in strain EP155 were set as 1.0 and the transcript levels of the corresponding genes in the hypovirus-infected strain EP713 were expressed as folds relative to those in EP155. Bars indicate mean deviation for three independent assays. Asterisk (*) means no significant change at mRNA level or opposite changing trend for mRNA and protein.

3.2 低毒病毒侵染对宿主体内甲基化的促进作用

在本研究中,作者第一次发现了两种均被注释为依赖于腺苷甲硫氨酸的甲基转移酶(S-adenosylmethionine-dependent methyltransferase, 编号 38、86、152,其中蛋白点 38 和 152 为同一种蛋白质)的未知蛋白在病毒侵染后均发生过量表达现象(图 1-D)。该现象与板栗疫病菌受低毒病毒侵染后,腺苷蛋氨酸合成酶(S-adenosyl-L-methionine synthetase, SAMS)和高半胱氨酸脱氢酶(S-adenosyl-

L-homocysteine hydrolase, SAHH) mRNA 的过量累积情况极其类似^[18-27],表明病毒侵染对宿主体内甲基化进程有促进作用。生物体内甲基化是一个很长的过程,通过超过 40 种代谢反应,将甲基从腺苷蛋氨酸(S-adenosyl-L-methionine, SAM)上转移到包括核苷酸、蛋白质、脂肪在内的各种基质上。在维生素 B2、B6、B12 存在的条件下,SAM 失去甲基后将形成高半胱氨酸(S-adenosyl-L-homocysteine, SAH)。转甲基作用的提高,可能引发一系列的代谢和生理变

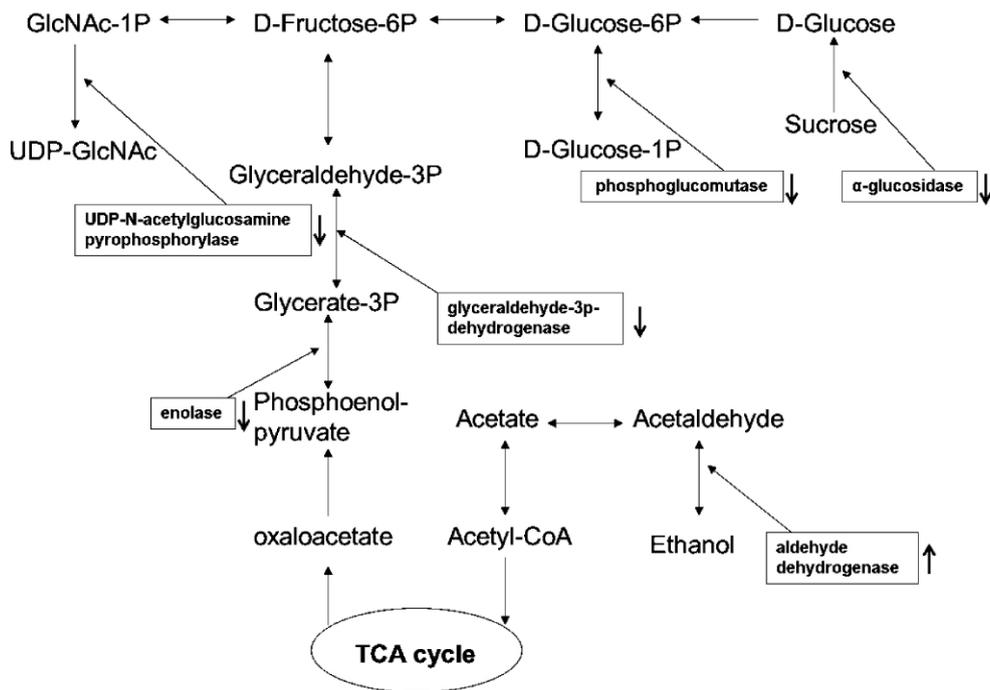


图 3. 低毒病毒侵染对 TCA 循环关联途径关键酶的调控示意图

Figure 3. Diagram of key enzymes in TCA cycle regulated by hypovirus infection. “↑” indicates up-regulated and “↓” down-regulated by hypovirus.

化,例如高浓度的 SAM 将影响蛋白质的合成及生物膜完整性^[18]。根据现有的研究结果推测,违反常规的生物体内甲基化反应将会导致大范围基因的表达调控紊乱^[28]。而对板栗疫病菌 SAHH 基因功能的研究,也证实了甲基化途径中关键基因的不正常表达会导致真菌低毒力现象的产生,与病毒侵染导致的致病力下降情况完全一致^[29]。

3.3 低毒病毒侵染对宿主热休克蛋白的调控

在受低毒病毒侵染的板栗疫病菌总蛋白组中,两种热休克蛋白 HSP30 和 HSP70 (图 1-D, 编号 37、63) 表达量显著上调。在粗糙脉孢菌 (*Neurospora crassa*) 中, HSP30 被认为与线粒体有关, 并且和 HSP88 发生相互作用^[30-31]。在动物和植物中, 已有病毒侵染导致宿主热休克蛋白表达量明显改变的报道^[32]。HSP70 被认为与病毒粒子的组装和病毒基因组的复制有关^[33]。值得一提的是, 在热休克蛋白家族中, 很多基因也是病毒必须的宿主因子, 例如 HSP90 与乙型肝炎病毒 (HBV) 的反转录酶作用, 促进病毒复制组装所必需的核蛋白复合体的形成^[34]; HSP90 与流感病毒 (influenza virus) RNA 聚合酶结合, 激活其活性, 使病毒 RNA 进入转录和复制过

程^[32]; HSP60 可以阻断 HBV 的复制^[35], 以及 HSP72 可以增强丙型肝炎病毒 (HCV) RNA 的复制^[36]。近年来对兽棚病毒 (flock house virus) 的研究发现, HSP70 和 HSP90 与病毒 RNA 的合成密切相关^[37-39]。作者在板栗疫病菌细胞器蛋白组研究中, 也找到了受病毒调控的热休克蛋白 (未发表)。因此, 在板栗疫病菌中发现的一系列差异表达的热休克蛋白, 很可能也是病毒的宿主因子。

3.4 低毒病毒侵染降低了真菌毒力因子 cyclophilin A 的积累量

受低毒病毒感染后, 板栗疫病菌的亲环素 (cyclophilin A) 表达量明显下调 (图 1-A, 编号 179)。在植物致病真菌稻瘟病菌的研究中发现, 由 CYP1 编码的 cyclophilin 具有调节毒力的功能, 影响附着胞的产生、脂肪的生物合成、无性孢子的发育^[40]。本实验室最近的研究表明, 敲除亲环素编码基因 *cyp1* 导致低毒力现象的产生, 同时与真菌毒力有关的信号传导途径也受到影^[22]。

3.5 低毒病毒调控宿主基因表达的多样性

对随机挑选的受病毒调控的部分宿主蛋白质的 mRNA 转录水平的定量分析显示, 并不是所有基因在转录水平和蛋白质水平都表现出相同的变化趋

势,其中有部分基因转录水平没有变化或呈现反向变化(图2)。通过将本研究得到的差异表达蛋白质数据与之前研究报道的 cDNA 芯片^[18]和 EST 文库^[24]信息进行比对分析,发现在匹配的 51 个蛋白质编码基因中,有 11 个表现出同样的变化趋势,9 个表现出相反的变化趋势,31 个基因在 mRNA 水平并没有发生变化。虽然本研究鉴定的差异表达蛋白质数据量有限,尚不能体现宿主在受到低毒病毒侵染后的蛋白组和转录组变化的全貌,但根据本文研究结果和以往研究数据的对比结果,依然可以比较肯定地得到如下结论:低毒病毒侵染对板栗疫病菌基因的调控不仅发生在转录组层面,也可以发生在蛋白质翻译或翻译后蛋白质的加工修饰层面。这一发现对今后深入研究低毒病毒与板栗疫病菌的互作以及植物病原真菌的致病机理有指导意义。

参考文献

- [1] Nuss DL. Hypovirulence: mycoviruses at the fungal-plant interface. *Nature Reviews Microbiology*, 2005, 3 (8) : 632-642.
- [2] Anagnostakis SL. Biological control of chestnut blight. *Science*, 1982, 215 (4532) : 466-471.
- [3] Chen B, Craven MG, Choi GH, Nuss DL. cDNA-derived hypovirus RNA in transformed chestnut blight fungus is spliced and trimmed of vector nucleotides. *Virology*, 1994, 202 (1) : 441-448.
- [4] Nuss DL. Biological control of chestnut blight: an example of virus-mediated attenuation of fungal pathogenesis. *Microbiological Reviews*, 1992, 56 (4) : 561-576.
- [5] Chen B, Gao S, Choi GH, Nuss DL. Extensive alteration of fungal gene transcript accumulation and elevation of G-protein-regulated cAMP levels by a virulence-attenuating hypovirus. *Proceedings of the National Academy of Sciences of the United States of America*, 1996, 93 (15) : 7996-8000.
- [6] Dawe AL, Nuss DL. Hypoviruses and chestnut blight: exploiting viruses to understand and modulate fungal pathogenesis. *Annual Review of Genetics*, 2001, 35 : 1-29.
- [7] Choi GH, Chen B, Nuss DL. Virus-mediated or transgenic suppression of a G-protein alpha subunit and attenuation of fungal virulence. *Proceedings of the National Academy of Sciences of the United States of America*, 1995, 92 (1) : 305-309.
- [8] Gao S, Nuss DL. Distinct roles for two G protein alpha subunits in fungal virulence, morphology, and reproduction revealed by targeted gene disruption. *Proceedings of the National Academy of Sciences of the United States of America*, 1996, 93 (24) : 14122-14127.
- [9] Parsley TB, Chen B, Geletka LM, Nuss DL. Differential modulation of cellular signaling pathways by mild and severe hypovirus strains. *Eukaryotic Cell*, 2002, 1 (3) : 401-413.
- [10] Choi ES, Chung HJ, Kim MJ, Park SM, Cha BJ, Yang MS, Kim DH. Characterization of the ERK homologue Cpmk2 from the chestnut blight fungus *Cryphonectria parasitica*. *Microbiology*, 2005, 151 (Pt 5) : 1349-1358.
- [11] Rostagno L, Prodi A, Turina M. Cpkk1, MAPKK of *Cryphonectria parasitica*, is necessary for virulence on chestnut. *Phytopathology*, 2010, 100 (10) : 1100-1110.
- [12] Turina M, Zhang L, Van Alfen NK. Effect of *Cryphonectria hypovirus 1* (CHV1) infection on Cpkk1, a mitogen-activated protein kinase kinase of the filamentous fungus *Cryphonectria parasitica*. *Fungal Genetics and Biology*, 2006, 43 (11) : 764-774.
- [13] Larson TG, Choi GH, Nuss DL. Regulatory pathways governing modulation of fungal gene expression by a virulence-attenuating mycovirus. *The EMBO Journal*, 1992, 11 (12) : 4539-4548.
- [14] Wang J, Wang F, Feng Y, Mi K, Chen Q, Shang J, Chen B. Comparative vesicle proteomics reveals selective regulation of protein expression in chestnut blight fungus by a hypovirus. *Journal of Proteomics*, 2013, 78 : 221-230.
- [15] Kim JM, Park JA, Kim DH. Comparative proteomic analysis of chestnut blight fungus, *Cryphonectria parasitica*, under tannic-acid-inducing and hypovirus-regulating conditions. *Canadian Journal of Microbiology*, 2012, 58 (7) : 863-871.
- [16] Yan JX, Wait R, Berkelman T, Harry RA, Westbrook JA, Wheeler CH, Dunn MJ. A modified silver staining protocol for visualization of proteins compatible with matrix-assisted laser desorption/ionization and electrospray ionization-mass spectrometry. *Electrophoresis*, 2000, 21 (17) : 3666-3672.
- [17] Gharahdaghi F, Weinberg CR, Meagher DA, Imai BS, Mische SM. Mass spectrometric identification of proteins from silver-stained polyacrylamide gel: a method for the removal of silver ions to enhance sensitivity.

Electrophoresis, 1999, 20 (3) : 601-605.

- [18] Allen TD, Dawe AL, Nuss DL. Use of cDNA microarrays to monitor transcriptional responses of the chestnut blight fungus *Cryphonectria parasitica* to infection by virulence-attenuating hypoviruses. *Eukaryotic Cell*, 2003, 2 (6) : 1253-1265.
- [19] Livak KJ, Schmittgen TD. Analysis of relative gene expression data using real-time quantitative PCR and the 2^{-ΔΔC_T} Method. *Methods*, 2001, 25 (4) : 402-408.
- [20] Choi GH, Nuss DL. Nucleotide sequence of the glyceraldehyde-3-phosphate dehydrogenase gene from *Cryphonectria parasitica*. *Nucleic Acids Research*, 1990, 18 (18) : 5566.
- [21] Razanamparany V, Jara P, Legoux R, Delmas P, Msayeh F, Kaghad M, Loison G. Cloning and mutation of the gene encoding endothiasepsin from *Cryphonectria parasitica*. *Current Genetics*, 1992, 21 (6) : 455-461.
- [22] Chen MM, Jiang M, Shang J, Lan X, Yang F, Huang J, Nuss DL, Chen B. CYP1, a hypovirus-regulated cyclophilin, is required for virulence in the chestnut blight fungus. *Molecular Plant Pathology*, 2011, 12 (3) : 239-246.
- [23] Dawe AL, McMains VC, Panglao M, Kasahara S, Chen B, Nuss DL. An ordered collection of expressed sequences from *Cryphonectria parasitica* and evidence of genomic microsynteny with *Neurospora crassa* and *Magnaporthe grisea*. *Microbiology*, 2003, 149 (Pt 9) : 2373-2384.
- [24] Shang J, Wu X, Lan X, Fan Y, Dong H, Deng Y, Nuss DL, Chen B. Large-scale expressed sequence tag analysis for the chestnut blight fungus *Cryphonectria parasitica*. *Fungal Genetics and Biology : FG & B*, 2008, 45 (3) : 319-327.
- [25] Hua Q, Yang C, Baba T, Mori H, Shimizu K. Responses of the central metabolism in *Escherichia coli* to phosphoglucose isomerase and glucose-6-phosphate dehydrogenase knockouts. *Journal of Bacteriology*, 2003, 185 (24) : 7053-7067.
- [26] Dawe AL, Van Voorhies WA, Lau TA, Ulanov AV, Li Z. Major impacts on the primary metabolism of the plant pathogen *Cryphonectria parasitica* by the virulence-attenuating virus CHV1-EP713. *Microbiology*, 2009, 155 (Pt 12) : 3913-3921.
- [27] Allen TD, Nuss DL. Specific and common alterations in host gene transcript accumulation following infection of the chestnut blight fungus by mild and severe hypoviruses. *Journal of Virology*, 2004, 78 (8) : 4145-4155.
- [28] Zhang X, Yazaki J, Sundaresan A, Cokus S, Chan SW, Chen H, Henderson IR, Shinn P, Pellegrini M, Jacobsen SE, Ecker JR. Genome-wide high-resolution mapping and functional analysis of DNA methylation in arabidopsis. *Cell*, 2006, 126 (6) : 1189-1201.
- [29] Liao S, Li R, Shi L, Wang J, Shang J, Zhu P, Chen B. Functional analysis of an S-adenosylhomocysteine hydrolase homolog of chestnut blight fungus. *FEMS Microbiology Letters*, 2012, 336 (1) : 64-72.
- [30] Plesofsky-Vig N, Brambl R. Characterization of an 88-kDa heat shock protein of *Neurospora crassa* that interacts with Hsp30. *The Journal of Biological Chemistry*, 1998, 273 (18) : 11335-11341.
- [31] Plesofsky-Vig N, Brambl R. Gene sequence and analysis of hsp30, a small heat shock protein of *Neurospora crassa* which associates with mitochondria. *The Journal of Biological Chemistry*, 1990, 265 (26) : 15432-15440.
- [32] Aranda MA, Escaler M, Wang D, Maule AJ. Induction of HSP70 and polyubiquitin expression associated with plant virus replication. *Proceedings of the National Academy of Sciences of the United States of America*, 1996, 93 (26) : 15289-15293.
- [33] Cripe TD, SE. Estes, PA. Garcea, RL. In vivo and in vitro association of hsc70 with polyomavirus capsid proteins. *Journal of Virology*, 1995, 69 (12) : 7807-7813.
- [34] Hu J, Seeger C. Hsp90 is required for the activity of a hepatitis B virus reverse transcriptase. *Proceedings of the National Academy of Sciences of the United States of America*, 1996, 93 (3) : 1060-1064.
- [35] Park SG, Lee SM, Jung G. Antisense oligodeoxynucleotides targeted against molecular chaperonin Hsp60 block human hepatitis B virus replication. *The Journal of Biological Chemistry*, 2003, 278 (41) : 39851-39857.
- [36] Chen YJ, Chen YH, Chow LP, Tsai YH, Chen PH, Huang CY, Chen WT, Hwang LH. Heat shock protein 72 is associated with the hepatitis C virus replicase complex and enhances viral RNA replication. *The Journal of Biological Chemistry*, 2010, 285 (36) : 28183-28190.
- [37] Castorena KM, Weeks SA, Stapleford KA, Cadwallader AM, Miller DJ. A functional heat shock protein 90 chaperone is essential for efficient flock house virus RNA polymerase synthesis in *Drosophila* cells. *Journal of*

Virology, 2007, 81 (16) : 8412-8420.

- [38] Weeks SA, Miller DJ. The heat shock protein 70 cochaperone YDJI is required for efficient membrane-specific flock house virus RNA replication complex assembly and function in *Saccharomyces cerevisiae*. *Journal of Virology*, 2008, 82 (4) : 2004-2012.
- [39] Weeks SA, Shield WP, Sahi C, Craig EA, Rospert S,

Miller DJ. A targeted analysis of cellular chaperones reveals contrasting roles for heat shock protein 70 in flock house virus RNA replication. *Journal of Virology*, 2010, 84 (1) : 330-339.

- [40] Viaud MC, Balhadere PV, Talbot NJ. A *Magnaporthe grisea* cyclophilin acts as a virulence determinant during plant infection. *Plant Cell*, 2002, 14 (4) : 917-930.

Proteomic analysis of *Cryphonectria parasitica* infected by a virulence-attenuating hypovirus

Jinzi Wang^{1,2}, Lidan Lu¹, Yanyan Yang¹, Qi Chen¹, Baoshan Chen^{1,3*}

¹College of Life Science and Technology, ²Agricultural College, ³State Key Laboratory for Conservation and Utilization of Subtropical Agro-bioresources, Guangxi University, Nanning 530005, Guangxi Zhuang Autonomous Region, China

Abstract: [Objective] Chestnut blight fungus *Cryphonectria parasitica* and hypovirus constitute a model system to study fungal pathogenesis and host-virus interaction. Proteomic analysis of chestnut blight fungus upon hypovirus infection was conducted to find the differentially expressed host proteins. [Methods] According to the characteristics of this filamentous fungus, an optimized extraction protocol for fungal total protein was developed. Two-dimensional electrophoresis (2-DE) was used for comparative proteomic analysis of wild strain EP155 and hypovirus-infected strain EP713. The quantitative RT-PCR was applied to analyze mRNA expression level of protein-coding genes. [Results] In total 71 protein spots were detected to be differentially expressed on the base of EP155 of which 19 up-regulated and 52 down-regulated. Fifty-eight unique proteins were identified by mass spectrometry. Further study on quantitative RT-PCR indicated that the regulation of related host genes by hypovirus occurred at different levels. [Conclusion] The TCA cycle of *C. parasitica* was weakened after hypovirus infection and the process of methylation was regulated by hypovirus. Meanwhile, viral regulation of virulence factors also contributed to the phenomenon of hypovirulence.

Keywords: *Cryphonectria parasitica*, hypovirus, comparative proteome

(本文责编:王晋芳)

Supported by the National Natural Science Foundation of China (39925003, 31170137, 31370173)

* Corresponding author. Tel: +86-771-3225260; Fax: +86-771-3237873; E-mail: chenyaoj@gxu.edu.cn

Received: 18 November 2013 / Revised: 9 March 2014